~0.12 for this grain is higher than any reported to date in presolar oxide grains (*30*, *33*, *34*). However, shell H-burning and third dredge-up in low-mass AGB stars produce a $^{26}Al/^{27}Al$ ratio of only $\sim 1.5 \times 10^{-3}$ in the envelope (*26*). Another consideration is that the grain has to form before dredge-up of C turns the star into a carbon star (*23*). Consequently, another process must be invoked to account for the large $^{26}Al/^{27}Al$. Previously, CBP was invoked to account for the high $^{26}Al/^{27}Al$ ratios found in a corundum and a hibonite grain (*34*). As mentioned already, CBP occurs in low-mass stars during the RGB and the thermally pulsing AGB phases. Although CBP alters the O and Al isotopic abundances simultaneously, there is no correlation between the two systems because the decrease in $^{18}O/^{16}O$ is dependent on the rate of mass circulation ($\dot{M}$), whereas $^{26}Al/^{27}Al$ depends on the maximum temperature of the circulated material (T_P), which in turn depends on depth of penetration (*23*). According to CBP models for a 1.5 $M_\odot$ (solar mass) star (*23*), ^{26}Al is abundantly produced for $\log T_P > 7.65$, but the large $^{26}Al/^{27}Al$ observed in the presolar silicate grain requires $\log T_P > 7.76$ and very deep mixing. In addition, the O isotopic composition of this grain requires $\dot{M} > 10^{-6}\ M_\odot$ per year. These values for T_P and $\dot{M}$ are feasible in low-mass thermally pulsing AGB stars undergoing CBP. It is apparent that the combined isotopic analysis of O and Mg provides more detailed information on deep mixing processes than just one isotopic system would provide.

In combining the data for all presolar silicates in IDPs (*11*, *12*), we arrive at a total abundance of ~890 ppm (*9*). In contrast, the abundance in Acfer 094 relative to the matrix material is ~40 ppm. This difference confirms that IDPs are more primitive than any meteorite. The abundance of circumstellar silicates in the matrix of the ordinary chondrites Semarkona and Bishunpur has been inferred to be ~15 ppm (*14*, *15*) compared with ~40 ppm in Acfer 094. These ordinary chondrites have undergone more aqueous alteration than Acfer 094 and formed at higher temperatures. This difference in abundance gives us a first look at the effects of meteorite formation histories and parent body processes on presolar grain survival. Determination of the abundances of presolar silicates in other meteorite classes will give us a means of studying the physical conditions in different solar system environments. Due to the unusually primitive nature of Acfer 094, we do not expect the abundance to be higher in other meteorites, but we still do not understand the destructive processes affecting presolar silicate grains well enough to make this a firm prediction.

References and Notes

1. E. Zinner, in *Meteorites, Comets, and Planets*, A. M. Davis, Ed. (Elsevier, Oxford, UK, 2004), vol. 1, pp. 17–39.
2. C. Waelkens *et al.*, *Astron. Astrophys.* **315**, L245 (1996).
3. K. Malfait *et al.*, *Astron. Astrophys.* **332**, L25 (1998).
4. L. B. F. M. Waters *et al.*, *Astron. Astrophys.* **315**, L361 (1996).
5. K. Demyk, E. Dartois, H. Wiesemeyer, A. P. Jones, L. d'Hendecourt, *Astron. Astrophys.* **364**, 170 (2000).
6. L. R. Nittler, thesis, Washington University (1996).
7. S. Messenger, T. J. Bernatowicz, *Meteorit. Planet. Sci.* **35**, A109 (2000).
8. C. M. O'D. Alexander, L. Nittler, F. Tera, *Lunar Planet. Sci.* **XXXII**, A2191 (2001).
9. Materials and methods are available as supporting material on *Science* Online.
10. A. Nguyen, E. Zinner, R. S. Lewis, *Publ. Astron. Soc. Aust.* **20**, 382 (2003).
11. S. Messenger, L. P. Keller, F. J. Stadermann, R. M. Walker, E. Zinner, *Science* **300**, 105 (2003).
12. C. Floss, F. J. Stadermann, *Lunar Planet. Sci.* **XXXV**, A1281 (2004).
13. J. P. Bradley, *Science* **265**, 925 (1994).
14. S. Mostefaoui, P. Hoppe, K. K. Marhas, E. Gröner, *Meteorit. Planet. Sci.* **38**, A99 (2003).
15. S. Mostefaoui, K. K. Marhas, P. Hoppe, *Lunar Planet. Sci.* **XXXV**, A1593 (2004).
16. F. J. Molster, L. B. F. M. Waters, A. G. G. M. Tielens, C. Koike, H. Chihara, *Astron. Astrophys.* **382**, 241 (2002).
17. F. J. Molster *et al.*, *Nature* **401**, 563 (1999).
18. S. Weinbruch, H. Palme, W. F. Müller, A. El Goresy, *Meteoritics* **25**, 115 (1990).
19. X. Hua, J. Adam, A. El Goresy, H. Palme, *Geochim. Cosmochim. Acta* **52**, 1389 (1988).
20. E. Zinner, *Annu. Rev. Earth Planet. Sci.* **26**, 147 (1998).
21. A. I. Boothroyd, I.-J. Sackmann, *Astrophys. J.* **510**, 232 (1999).
22. G. J. Wasserburg, A. I. Boothroyd, I.-J. Sackmann, *Astrophys. J.* **447**, L37 (1995).
23. K. M. Nollett, M. Busso, G. J. Wasserburg, *Astrophys. J.* **582**, 1036 (2003).
24. A. I. Boothroyd, I.-J. Sackmann, G. J. Wasserburg, *Astrophys. J.* **442**, L21 (1995).
25. R. C. Cannon, C. A. Frost, J. C. Lattanzio, P. R. Wood, in *Nuclei in the Cosmos III*, M. Busso, R. Gallino, C. M. Raiteri, Eds. (AIP, New York, 1995), pp. 469–472.
26. M. Forestini, G. Paulus, M. Arnould, *Astron. Astrophys.* **252**, 597 (1991).
27. N. Mowlavi, G. Meynet, *Astron. Astrophys.* **361**, 959 (2000).
28. A. I. Karakas, J. C. Lattanzio, *Publ. Astron. Soc. Aust.* **20**, 279 (2003).
29. M. Busso, R. Gallino, G. J. Wasserburg, *Annu. Rev. Astron. Astrophys.* **37**, 239 (1999).
30. L. R. Nittler, C. M. O'D. Alexander, X. Gao, R. M. Walker, E. Zinner, *Astrophys. J.* **483**, 475 (1997).
31. C. M. O'D. Alexander, L. R. Nittler, *Astrophys. J.* **519**, 222 (1999).
32. B.-G. Choi, G. R. Huss, G. J. Wasserburg, R. Gallino, *Science* **282**, 1284 (1998).
33. I. D. Hutcheon, G. R. Huss, A. J. Fahey, G. J. Wasserburg, *Astrophys. J.* **425**, L97 (1994).
34. B.-G. Choi, G. J. Wasserburg, G. R. Huss, *Astrophys. J.* **522**, L133 (1999).

35. We thank the reviewer for valuable comments and are grateful to S. Amari and C. Floss for their assistance with SEM measurements and helpful discussions. We also thank S. Messenger and F. Stadermann for developing the software for processing the isotopic images. Supported by NASA grants NAG5-10426 and NAG5-11545.

Supporting Online Material

www.sciencemag.org/cgi/content/full/303/5663/1496/DC1
Materials and Methods
Table S1
References

5 December 2003; accepted 30 January 2004

European Seasonal and Annual Temperature Variability, Trends, and Extremes Since 1500

Jürg Luterbacher,[1,2]* Daniel Dietrich,[3] Elena Xoplaki,[2] Martin Grosjean,[1] Heinz Wanner[1,2]

Multiproxy reconstructions of monthly and seasonal surface temperature fields for Europe back to 1500 show that the late 20th- and early 21st-century European climate is very likely (>95% confidence level) warmer than that of any time during the past 500 years. This agrees with findings for the entire Northern Hemisphere. European winter average temperatures during the period 1500 to 1900 were reduced by ~0.5°C (0.25°C for annual mean temperatures) compared to the 20th century. Summer temperatures did not experience systematic century-scale cooling relative to present conditions. The coldest European winter was 1708/1709; 2003 was by far the hottest summer.

Detailed insight into high-resolution temporal and spatial patterns of climate change during previous centuries is essential for assessing the degree to which late 20th-century changes may be unusual in the light of preindustrial natural climate variability (*1–3*). Climate change at seasonal to annual resolutions for recent centuries has been highlighted in a number of studies, which have included climate modeling experiments with estimated natural and anthropogenic radiative-forcing changes (*4–6*) and empirical hemispheric or global reconstructions. Such reconstructions are based either on natural archives only (such as ice cores, tree rings, speleothems, varved sediments, and subsurface temperature profiles obtained from borehole measurements) or on multiproxy networks that amalgamate natural proxy indicators with climate information obtained from early instrumental and documentary evidence (*7–14*). A number of these reconstructions support the conclusion that the warmth of the late 20th century is likely unprecedented in the Northern

[1]National Center of Competence in Research (NCCR) Climate, [2]Institute of Geography, Climatology, and Meteorology, [3]Department of Mathematical Statistics and Actuarial Science, University of Bern, CH–3012 Bern, Switzerland.

*To whom correspondence should be addressed. E-mail: juerg@giub.unibe.ch

Hemisphere in the past 1000 years and cannot be explained by natural forcings alone (*15*).

Hemispheric and global temperature reconstructions do not provide information about regional-scale variations, such as the intrinsic seasonal patterns of climate change as they have occurred in Europe during the past centuries. The few European-scale temperature reconstructions (*7*, *16*–*19*) have revealed information for the winter or summer half-year or for annual to multiannual mean values. Changes in the full annual cycle have typically not been addressed, because of the limited year-round information provided by most natural climate proxy data (*2*, *20*).

Regional and temporal high-resolution reconstructions also illuminate key climatic features, such as regionally very hot or cool summers and very mild or cold winters, that may be masked in a hemispheric or global reconstruction (*15*, *16*). Thus, regional studies and reconstructions of climate change are critically important when climate impacts are evaluated (*21*–*23*). Extremes at regional scales, such as the hot summer of 2003 in many European areas, exhibit much larger amplitudes than extremes at the global scale, and they may thus markedly affect the local to regional natural environment, society, and economy, including most vital aspects such as water supply and agriculture.

Here we present a new gridded (0.5° × 0.5° resolution) reconstruction of monthly (back to 1659) and seasonal (from 1500 to 1658) temperature fields for European land areas (25°W to 40°E and 35°N to 70°N) (*19*). This reconstruction is based on a comprehensive data set that includes a large number of homogenized and quality-checked instrumental data series, a number of reconstructed sea-ice and temperature indices derived from documentary records for earlier centuries, and a few seasonally resolved proxy temperature reconstructions from Greenland ice cores and tree rings from Scandinavia and Siberia (fig. S1 and tables S1 and S2). We discuss the evolution of European winter, summer, and annual mean temperatures for more than 500 years in the context of estimated uncertainties, emphasizing the trends, spatial patterns for extreme summers and winters, and changes in both extreme and mean conditions.

Fig. 1A presents the winter [December through February (DJF)] European surface temperature variations since 1500 (relative to the 1901 to 1995 average) and the 95% confidence range [±2 standard error (SE)] (*19*). The uncertainty is larger in the earlier reconstructions. From the 16th to the beginning of the 18th century, the two SEs of the filtered wintertime series are in the order of 1.3°C, and they reduce to 0.4°C from 1865 onwards. The larger uncertainties in the earlier centuries are mainly due to a smaller number of uniformly distributed instrumental records (none before 1659), but are also due to fewer proxy series and additional uncertainties in the documentary data (*20*, *24*–*26*) and natural proxies (*2*, *27*).

Except for two short periods around 1530 and 1730, European winters were generally colder than those of the 20th century. The coldest multidecadal winter periods were experienced during the late 16th century, during the last decades of the 17th century, and at the end of the 19th century (ΔT = ~–0.8°C, where ΔT is the change from the 1901 to 1995 average). The winter of 1708/1709 was the coldest in record (ΔT = –3.6°C) and probably related to a negative North Atlantic Oscillation (NAO) index (*28*–*30*). We reconstructed spatial anomaly patterns of the three individual months and the average of winter 1708/1709 (Fig. 2A). January and February contributed most to the overall cold when temperatures over large parts of Europe and western Russia were more than 7°C below average. Except for the northernmost part of our study area, the reconstruction is reliable. Independent climate evidence from different European areas confirms the existence of strong negative temperature anomalies (supporting online text).

We calculated the return period of a European-wide event such as the coldest winter of 1708/1709. This calculation is based on fitting a spline function and is sensitive to the trend over the period 1750 to 2002 and the assumption of Gaussian distributed residuals (*19*). We obtained a return period of 200 to 500 years for winter conditions from 1750 to ~1900. The warming of the 20th century leads to an increase in the return period, which amounts to more than 100,000 years at the turn of the 21st century (fig. S2A). However, the uncertainties of the estimates are large, and the return periods should be considered with caution (fig. S2A).

Fig. 2C presents anomaly (1901 to 1995 average subtracted) composites and the corresponding standard deviations (SDs) for the ten coldest European winters, excluding 1708/1709. The anomaly composite resembles the 1708/1709 winter. It indicates continental cold with the largest deviations and highest variability over northern and eastern Europe, western

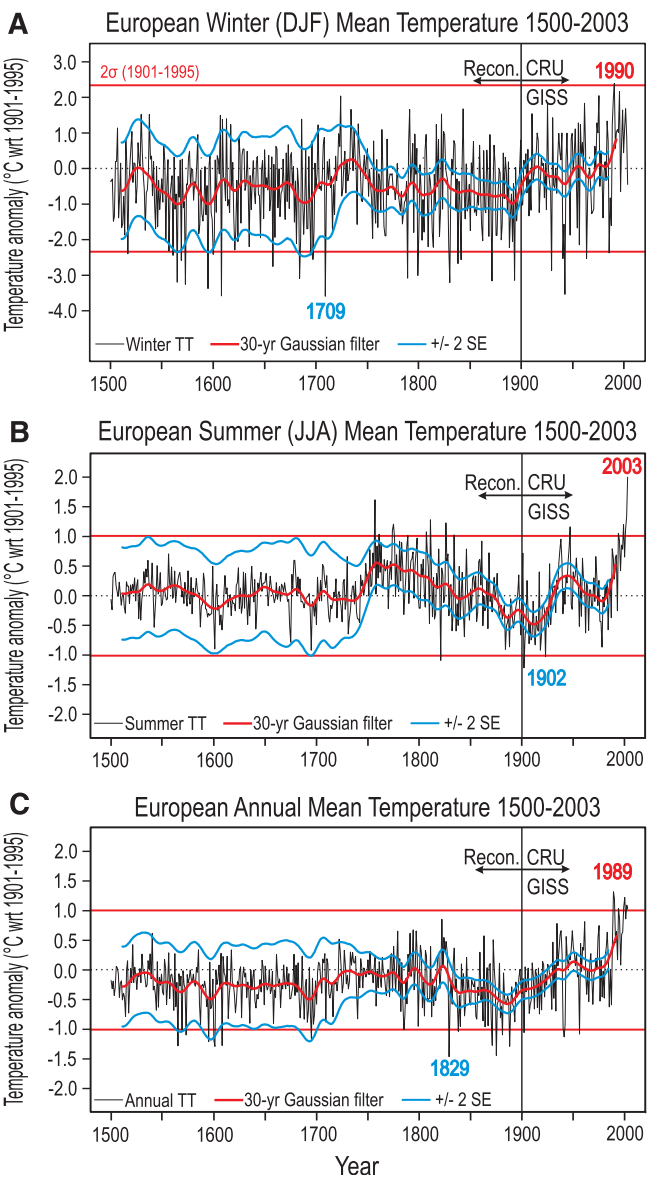

Fig. 1. (**A**) Winter (DJF), (**B**) summer (JJA), and (**C**) annual averaged-mean European temperature anomaly (relative to the 1901 to 1995 calibration average) time series from 1500 to 2003, defined as the average over the land area 25°W to 40°E and 35°N to 70°N (thin black line). The values for the period 1500 to 1900 are reconstructions; data from 1901 to 1998 are derived from (*44*). The post-1998 data stem from (*45*); Goddard Institute for Space Studies (GISS) NASA surface temperature analysis is given on a 1° × 1° resolution (*46*). Temperature data from (*44*) and (*45*) are very similar and correlate at 0.98 for each season within the common period 1901 to 1998 for the chosen area; they do not indicate any absolute bias. The thick red line is a 30-year Gaussian low-pass filtered time series. Blue lines show the ±2 SEs of the filtered reconstructions on either side of the low-pass filtered values. The red horizontal lines are the 2-SD line of the period 1901 to 1995. The warmest and the coldest winters, summers, and years are denoted in blue and red, respectively. The winter *y* axis uses a different scale. Recon., reconstructed; CRU, Climatic Research Unit (*44*); TT, temperature; wrt, as compared to.

Russia, and Scandinavia, and positive anomalies over Iceland and parts of Turkey. It shows the well-known seesaw in winter temperature between Greenland/Iceland and Europe (*31*), associated with large-scale variations in the atmosphere–ocean–sea ice system.

A strong winter warming trend was observed between 1684 and 1738. The linear trend for this period amounts to +0.32°C ± 0.18°C per decade. (All confidence ranges on trends are calculated at the 95% confidence level and are statistically significant.) Such an intense increase in European winter temperature over a comparable time period was not observed elsewhere in the 500-year record. The spatial trend map for this 55-year period (Fig. 3) indicates an increasing warming gradient from southwestern to northeastern Europe, with maximum values (0.8°C per decade) over Scandinavia and the Baltic region. A strong trend toward decreased winter ice severity in the Western Baltic for the same period has been found (*32*), thus supporting our findings with independent climate information.

The large-scale European warming during this time may have been caused by different processes. In a stratosphere-resolving general circulation model (*22*, *33*), decadal-scale conti-

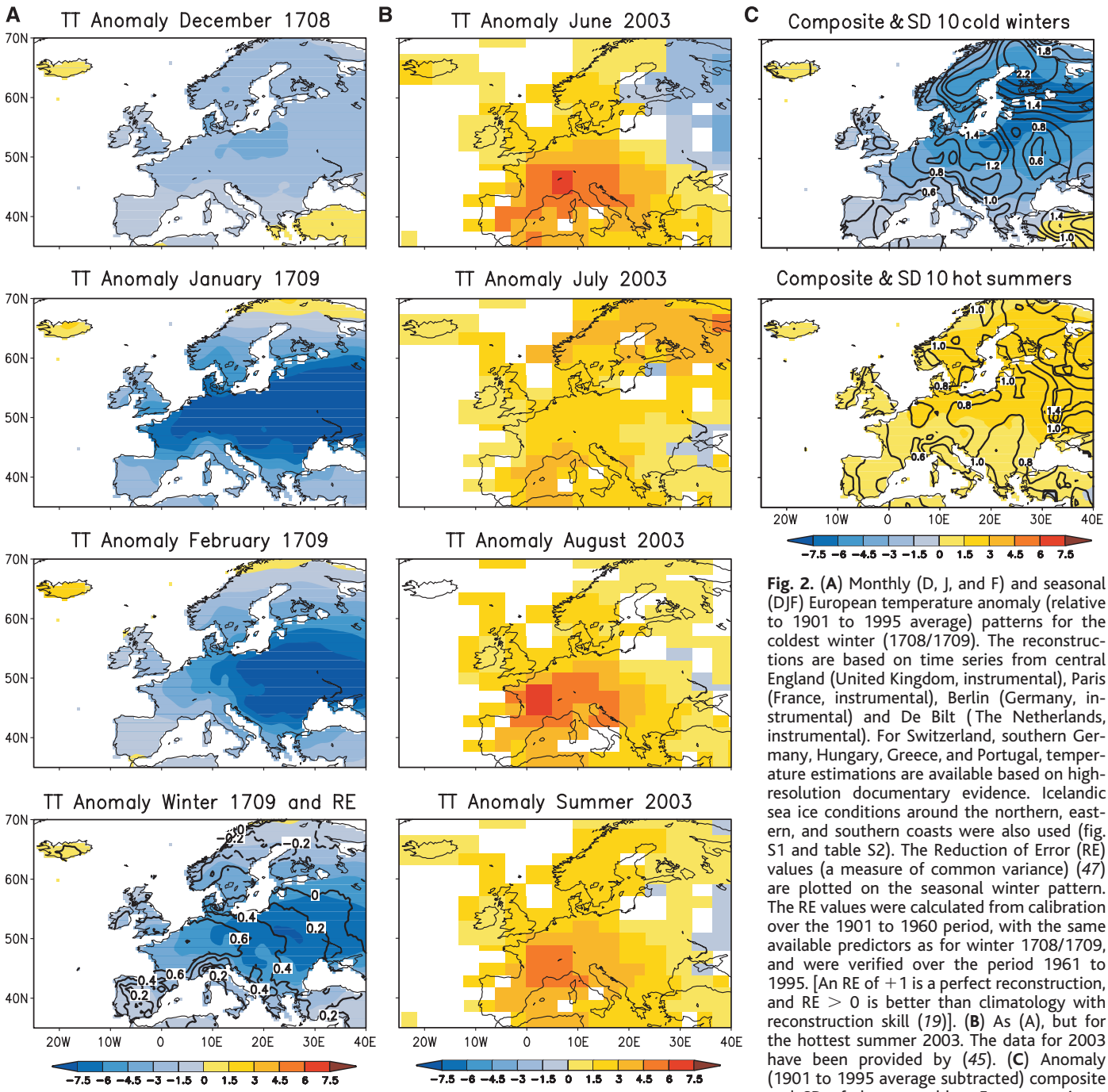

Fig. 2. (**A**) Monthly (D, J, and F) and seasonal (DJF) European temperature anomaly (relative to 1901 to 1995 average) patterns for the coldest winter (1708/1709). The reconstructions are based on time series from central England (United Kingdom, instrumental), Paris (France, instrumental), Berlin (Germany, instrumental) and De Bilt (The Netherlands, instrumental). For Switzerland, southern Germany, Hungary, Greece, and Portugal, temperature estimations are available based on high-resolution documentary evidence. Icelandic sea ice conditions around the northern, eastern, and southern coasts were also used (fig. S1 and table S2). The Reduction of Error (RE) values (a measure of common variance) (*47*) are plotted on the seasonal winter pattern. The RE values were calculated from calibration over the 1901 to 1960 period, with the same available predictors as for winter 1708/1709, and were verified over the period 1961 to 1995. [An RE of +1 is a perfect reconstruction, and RE > 0 is better than climatology with reconstruction skill (*19*)]. (**B**) As (A), but for the hottest summer 2003. The data for 2003 have been provided by (*45*). (**C**) Anomaly (1901 to 1995 average subtracted) composite and SD of the ten coldest European winters (excluding winter 1708/1709) and ten hottest summers (excluding summer 2003) over the period 1500 to 2003. Anomalies and SDs are given in °C. White grid cells indicate missing values. Extremely cold European winters are usually related to negative NAO situations and persistent high pressure systems centered over northern Europe or Scandinavia or to the westward extension of the Siberian anticyclone connected with continental easterly to northerly flow (*48*). Hot European summers are generally connected with a large number of persistent high-pressure systems over the continent, which may result in strong subsidence and/or warm air advection from the southwest. Dry soils can support the conversion of the surface radiation into heat (at the expense of evapotranspiration).

nental winter temperatures before the industrial era appear to respond differently to solar and volcanic forcings. Although both enhanced irradiance and large eruptions lead to continental warming, solar changes affect continental scales much more strongly, through forcing of the NAO or Arctic Oscillation (AO) [i.e., enhanced (reduced) solar irradiance causes a shift toward the high (low) index NAO/AO state]. Thus, solar forcing seems to dominate over volcanic eruptions, which induce a more homogeneous hemisphere-wide cooling at decadal time scales. Increased solar irradiance at the end of the 17th century and through the first half of the 18th century might have induced such a shift toward a high NAO/AO index, which agrees with independent proxy NAO reconstructions (*28*, *29*). It is well known that the NAO exerts a dominant influence on wintertime temperature over much of Europe, though the strength of the relationship can change over time and region (*34*). We confirm this behavior for the pre-instrumental period (*35*). Furthermore, North Atlantic sea surface temperatures (*36*) and tropical variability (*37*) are both relevant for NAO dynamics and might also be important for explaining the European winter warming during the late 17th and early 18th centuries. However, missing ocean data for this period impede testing of this hypothesis. Solar irradiance estimates stayed at relatively high values until the turn of the 19th century, whereas NAO index reconstructions and European winter temperatures indicate lower values. Mechanisms responsible for such European winter cooling are still under debate.

The linear winter temperature trend for the 20th century (1901 to 2000) is +0.08°C ± 0.07°C per decade. The winter 1989/1990 (ΔT = +2.4°C) and the decade 1989 to 1998 (ΔT = +1.2°C) were the warmest since 1500. The period 1989 to 1998 was almost two SEs warmer than the second warmest (nonoverlapping) decade (1733 to 1742, ΔT = +0.45°C), thus was very likely (95% confidence level) warmer than any other decade since 1500. At the multidecadal time scale (30-year averages), the winters between 1973 and 2002 were likely (85% probability) the warmest 30-year period of the last half-millennium. Winter 2002/2003, however, was 0.4°C colder than the 1901 to 1995 average. Recent findings (*38*) show that the effect of anthropogenic forcing is detectable on Eurasian winter temperatures over the period 1950 to 1999.

European summer [June through August (JJA)] temperatures are shown in Fig. 1B. The two-SE limits decrease from 0.7°C at 1500 to 0.2°C toward the end of the reconstruction period. A notable increase in reliability occurs in the first part of the 18th century, when instrumental data become available. Reconstructed European summers from ~1530 to 1570 were slightly warmer than the 1901 to 1995 average. A marked feature in the summer series is the higher temperatures from ~1750 until the second half of the 19th century, including the second hottest summer of 1757 (ΔT = +1.6°C). Importantly, possible inhomogeneities in the instrumental data before the mid-19th century cannot be fully excluded and are still a matter of discussion. For example, summer temperature observations from Stockholm and Uppsala (Sweden) could have been positively biased by as much as 0.7 to 0.8°C before ~1860, likely because of insufficient radiation protection of the thermometers (*39*). Reconstructed Northern Hemisphere summer temperatures (*12*) during this period remained below the 20th-century average. This underlines the fundamental difference between late 20th-century warming at the hemispherical scale and preindustrial regional warm episodes that were as warm or even warmer than today, but were limited in their geographical extent and scattered in their timing (*15*, *40*).

From 1757 onwards, there was a summer cooling trend (–0.06°C ± 0.02°C per decade) until the beginning of the 20th century, with 1902 as the coolest summer in the entire record. During the 20th century, the instrumental summer data depict first a warming trend until 1947, followed by a cooling trend until 1977. Subsequently, an exceptionally strong, unprecedented warming is observed (a linear trend of +0.7°C ± 0.20°C per decade) that featured very likely the hottest summer decade 1994 to 2003. The European summer temperatures show other multidecadal periods with comparable, though less strong, warming trends (1731 to 1757, 0.42°C ± 0.17°C per decade; 1923 to 1947, 0.45°C ± 0.23°C per decade, respectively). The summer of 2003 exceeded 1901 to 1995 European summer temperatures by around 2°C (4 SDs). Taking into account the uncertainties in our reconstructions, it appears that the summer of 2003 was very likely warmer than any other summer back to 1500.

The return period of a European-scale summer event exceeding 2°C (relative to the 1901 to 1995 average) was calculated with the same methodology (varying trend over time) as for the 1708/1709 winter (*19*). The return period is more than 5000 years for mid-18th century summer conditions (fig. S2B). It increases noticeably to millions of years at the turn of the 20th century and decreases to less than 100 years for the most recent summers (*19*). Schär *et al.* (*41*) found a much higher return period in their analysis of central European temperature. The differences might be related to the use of different methods, such as varying trend over time versus specified climatology, or of another base period connected with a different SD, as well as the different geographical area (regional versus continental). However, both estimates contain large uncertainties and should not be overinterpreted (fig. S2B) (*41*).

Results from regional climate model simulations (*41*, *42*) (under the Special Report on Emissions Scenarios A2, transient greenhouse-gas scenario) suggest that about every second summer will be as hot or even hotter than 2003 by the end of the 21st century (2071 to 2100). All individual summer months of 2003 (Fig. 2B) experienced significantly higher-than-normal temperatures, with maximum values over western and central Europe. The anomaly (1901 to 1995 average subtracted) composite of the ten hottest European summers (excluding 2003) (Fig. 2C) shows a monopole pattern with the most positive anomalies and highest variability over northeastern Europe.

The smoothed curve of European annual mean temperatures (Fig. 1C) clearly points to cooler conditions throughout the earlier reconstructed centuries. The 19th century (ΔT = –0.32°C) was the coldest of the last half-millennium. This agrees with reconstructions for the Northern Hemisphere (*9*). The coldest decadal periods were observed in the second part of the 19th century, at the end of the 17th century, and ~1600 (ΔT ~ –0.6°C), although with an increasing degree of uncertainty the earlier in time. Decadal-scale continental annual temperature changes during preindustrial times appear to be driven primarily by solar variability (*22*, *33*), although prolonged periods of volcanism could have also contributed to European cooling. Deforestation (*6*) may also be relevant for lower European annual temperatures in the late 19th century.

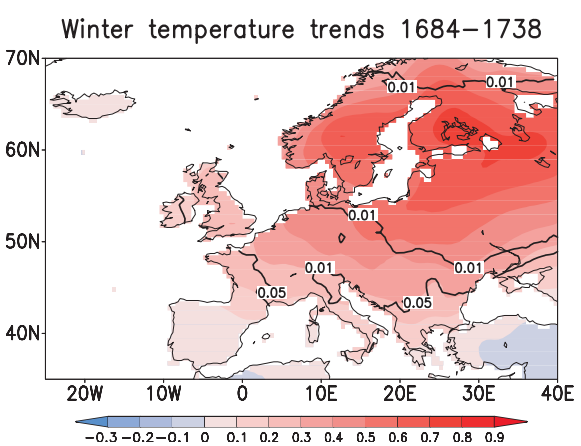

Fig. 3. Winter temperature trends (°C per decade) from 1684 to 1738. The thick solid lines represent the 95% and 99% confidence level (error probability 0.05 and 0.01), respectively, using a Mann-Kendall trend test. Except for the Mediterranean area, the warming trends are statistically significant over the whole of Europe.

The 20th century (1901 to 2000) was the warmest since 1500. There was a strong warming trend of +0.08°C ± 0.03°C per decade within the 20th century. The last 30 years (1974 to 2003, $\Delta T = +0.43$°C) were ~0.45°C higher than the second warmest 30-year periods (1722 to 1751 and 1750 to 1779) of the reconstructions. When we consider the uncertainties of earlier periods, the late 20th- and early 21st-century European warmth at multidecadal (30-year) scale is very likely unprecedented for more than the past 500 years. The nine warmest European years on record have occurred since 1989. The year 1989 ($\Delta T = +1.3$°C) and the decade 1994 to 2003 ($\Delta T = +0.84$°C) were very likely the warmest for more than half a millennium.

Our >500-year continental-scale surface temperatures provide evidence of current European climate change. Comparing recent temperature changes with those of the past and taking into account reconstruction uncertainties, we show that the late 20th- and early 21st-century warmth very likely exceeds that of any time during at least the past 500 years. The high-resolution reconstruction also sheds light on the spatial structure of regional temperature anomalies and extremes back in time. Furthermore, our temperature estimates provide a key test of the General Circulation Model's continental and seasonal response to different forcings (*22*, *43*).

References and Notes

1. M. E. Mann, R. S. Bradley, M. K. Hughes, *Nature* **392**, 779 (1998).
2. P. D. Jones, T. J. Osborn, K. R. Briffa, *Science* **292**, 662 (2001).
3. K. R. Briffa, T. J. Osborn, *Science* **295**, 2227 (2002).
4. T. J. Crowley, *Science* **289**, 270 (2000).
5. S. Gerber *et al.*, *Clim. Dyn.* **20**, 281 (2003).
6. E. Bauer, M. Claussen, V. Brovkin, A. Huenerbein, *Geophys. Res. Lett.* **30**, 1276 (2003).
7. R. S. Bradley, P. D. Jones, *Holocene* **3**, 367 (1993).
8. J. T. Overpeck *et al.*, *Science* **278**, 1251 (1997).
9. M. E. Mann, R. S. Bradley, M. K. Hughes, *Geophys. Res. Lett.* **26**, 759 (1999).
10. K. R. Briffa, *Quat. Sci. Rev* **19**, 87 (2000).
11. K. R. Briffa *et al.*, *J. Geophys. Res.* **106**, 2929 (2001).
12. P. D. Jones, K. R. Briffa, T. P. Barnett, S. F. B. Tett, *Holocene* **8**, 455 (1998).
13. J. Esper, E. R. Cook, F. H. Schweingruber, *Science* **295**, 2250 (2002).
14. M. E. Mann, S. Rutherford, R. S. Bradley, M. K. Hughes, F. T. Keimig, *J. Geophys. Res.* **108**, 4203 (2003).
15. M. E. Mann *et al.*, *Eos* **84**, 256 (2003).
16. M. E. Mann *et al.*, *Earth Interact.* **4-4**, 1 (2000).
17. J. Guiot, in *European Paleoclimate and Man, Paläoklimaforschung,* **7**, 93 (1991).
18. D. A. Fisher, *Holocene* **12**, 401 (2002).
19. Materials and methods are available as supporting material on *Science* Online.
20. P. D. Jones, K. R. Briffa, T. J. Osborn, *J. Geophys. Res.* **108**, 4588 (2003).
21. Z. W. Kundzewicz, M. L. Parry, in *Climate Change 2001: Impacts, Adaptation, and Vulnerability*, J. J. McCarthy *et al.*, Eds. (Cambridge Univ. Press, New York, 2001), pp. 641–692.
22. D. T. Shindell, G. A. Schmidt, R. L. Miller, M. E. Mann, *J. Clim.* **16**, 4094 (2003).
23. C. Pfister, in *Kulturelle Konsequenzen der Kleinen Eiszeit* [Cultural Consequences of the Little Ice Age], W. Behringer, H. Lehmann, C. Pfister, Eds. (Vandenhoek & Ruprecht, Göttingen), in press.
24. C. Pfister, *Wetternachhersage: 500 Jahre Klimavariationen und Naturkatastrophen 1496–1995* (Haupt-Verlag, Bern, 1999).
25. R. Brázdil, C. Pfister, H. Wanner, H. von Storch, J. Luterbacher, in preperation.
26. A. Pauling, J. Luterbacher, H. Wanner, *Geophys. Res. Lett.* **30**, 1787 (2003).
27. K. R. Briffa, T. J. Osborn, *Science* **284**, 926 (1999).
28. F. S. Rodrigo, D. Pozo-Vazquez, M. J. Esteban-Parra, Y. Castro-Diez, *J. Geophys. Res.* **106**, 14805 (2001).
29. E. R. Cook, R. D. D'Arrigo, M. E. Mann, *J. Clim.* **15**, 1754 (2002).
30. J. Luterbacher *et al.*, *Atmos. Sci. Lett.* **2**, 114 (2002).
31. H. van Loon, J. C. Rogers, *Mon. Wea. Rev.* **106**, 296 (1978).
32. G. Koslowski, R. Glaser, *Clim. Change* **41**, 175 (1999).
33. D. T. Shindell, G. A. Schmidt, M. E. Mann, D. Rind, A. M. Waple, *Science* **294**, 2149 (2001).
34. P. D. Jones, T. J. Osborn, K. R. Briffa, in *The North Atlantic Oscillation: Climatic Significance and Environmental Impact* [Geophysical Monograph 134], J. W. Hurrell, Y. Kushnir, G. Ottersen, M. Visbeck, Eds. (American Geophysical Union, Washington, DC, 2003).
35. J. Luterbacher, D. Dietrich, E. Xoplaki, M. Grosjean, H. Wanner, unpublished data.
36. M. J. Rodwell. D. P. Rowell, C. F. Folland, *Nature* **398**, 320 (1999).
37. J. W. Hurrell, M. P. Hoerling, A. S. Phillips, T. Xu, *Clim. Dyn.*, in press.
38. F. W. Zwiers, X. Zhang, *J. Clim.* **16**, 793 (2003).
39. A. Moberg, H. Alexandersson, H. Bergström, P. D. Jones, *Int. J. Climatol.* **23**, 1495 (2003).
40. R. S. Bradley, M. K. Hughes, H. F. Diaz, *Science* **302**, 404 (2003).
41. C. Schär *et al.*, *Nature* **427**, 332 (2004).
42. N. Nakicenovic *et al.*, *Intergovernmental Panel on Climate Change Special Report on Emissions Scenarios* (Cambridge Univ. Press, Cambridge, UK, 2000).
43. E. Zorita *et al.*, "Simulation of the climate of the last five centuries" (GKSS Report 2003/12, Geesthacht, Germany, 2003).
44. M. New, M. Hulme, P. D. Jones, *J. Clim.* **13**, 2217 (2000).
45. J. Hansen *et al.*, *J. Geophys. Res.* **106**, 23947 (2001).
46. Data are available at www.giss.nasa.gov/data/update/gistemp/.
47. E. R. Cook, K. R. Briffa, P. D. Jones, *Int. J. Climatol.* **14**, 379 (1994).
48. J. Luterbacher *et al.*, *Clim. Dyn.* **18**, 545 (2002).

49. We thank M. E. Mann, P. D. Jones, A. Moberg, F. J. González-Rouco, T. Jonsson, D. T. Shindell, T. F. Stocker, J. Esper, C. Pfister, N. Schneider, P. Della-Marta, A. Pauling, C. Casty, D. Oesch, E. Fischer, T. Rutishauser, P. Michna, and C. Neuhaus for discussions on various aspects of this paper; J. Hansen and R. Ruedy from NASA Goddard Institute for Space Studies for providing their surface temperature analysis; P. Michna for trend calculations; P. Della-Marta for English corrections; E. Fischer for the station network figure; E. Lerch for data extraction; and many other persons for providing their instrumental or proxy data. The authors are grateful for the use of predictor data from various sources. The Global Climate Data (Version 1, gridded temperature and precipitation) has been supplied by the Climate Impacts LINK Project (DEFRA, contract EPG 1/1/154) on behalf of the Climatic Research Unit, University of East Anglia. Supported by the Swiss National Science Foundation (NCCR Climate) (J.L.); the Fifth Framework Programme of the European Union [Project SOAP (Simulations, Observations and Paleoclimate Data: Climate Variability over the last 500 Years)] (E.X.); and the Bundesamt für Bildung und Wissenschaft under contract 01.0560 (B.B.W.).

Supporting Online Material

www.sciencemag.org/cgi/content/full/303/5663/1499/DC1
Materials and Methods
SOM Text
References and Notes
Figs. S1 and S2
Tables S1 and S2

20 November 2003; accepted 5 February 2004

Late Miocene Teeth from Middle Awash, Ethiopia, and Early Hominid Dental Evolution

Yohannes Haile-Selassie,[1]* Gen Suwa,[2] Tim D. White[3]

Late Miocene fossil hominid teeth recovered from Ethiopia's Middle Awash are assigned to *Ardipithecus kadabba*. Their primitive morphology and wear pattern demonstrate that *A. kadabba* is distinct from *Ardipithecus ramidus*. These fossils suggest that the last common ancestor of apes and humans had a functionally honing canine–third premolar complex. Comparison with teeth of *Sahelanthropus* and *Orrorin*, the two other named late Miocene hominid genera, implies that these putative taxa are very similar to *A. kadabba*. It is therefore premature to posit extensive late Miocene hominid diversity on the basis of currently available samples.

The phylogenetic status of the earliest hominid genera *Sahelanthropus*, *Orrorin*, and *Ardipithecus* (*1–6*) and the definition of the family Hominidae (*7–10*) are in debate. By what derived characters should the hominid (*1*, *11*) clade be recognized? Bipedality might be an arbiter of hominid status, but "bipedality" involves a large and complex set of anatomical traits and is not a dichotomous character. Femora attributed to *Orrorin tugenensis* at ~5.8 million years ago (Ma) constitute the earliest postcranial evidence for early hominid bipedality (*2*, *12*). However, the *O. tugenensis* femora are different from those of later hominids such as *Australopithecus afarensis* (*13*). Indeed, some question

[1]Cleveland Museum of Natural History, 1 Wade Oval Drive, Cleveland, OH 44106, USA. [2]The University Museum, The University of Tokyo, Bunkyo-Ku, Hongo, Tokyo 113-0033, Japan. [3]Department of Integrative Biology and Laboratory for Human Evolutionary Studies, Museum of Vertebrate Zoology, University of California, Berkeley, CA 94720, USA.

*To whom correspondence should be addressed. E-mail: yhailese@cmnh.org